Wiley Online Library
Early View publication on www.wileyonlinelibrary.com
(issue and page numbers not yet assigned;
citable using Digital Object Identifier – **DOI**)

Phys. Status Solidi A, 1–7 (2016) / **DOI** 10.1002/pssa.201600215

physica status solidi a
www.pss-a.com
applications and materials science

Part of Topical Section on
Recent Advances in Diamond Science and Technology

Fluorescence properties of nanodiamonds with NV centers in water suspensions

Alexey Vervald*[,1], Sergey Burikov, Nataliya Borisova[2], Igor Vlasov[3,4], Kirill Laptinskiy[1], Tatiana Laptinskaya[1], Olga Shenderova[5], and Tatiana Dolenko[1,4]

[1] Physical Department, M.V. Lomonosov Moscow State University, 119991 Moscow, Russia
[2] Chemical Department, M.V. Lomonosov Moscow State University, 119991 Moscow, Russia
[3] General Physics Institute, Russian Academy of Sciences, 119991 Moscow, Russia
[4] National Research Nuclear University MEPhI, 115409 Moscow, Russia
[5] Adamas Nanotechnologies Inc., 8100 Brownleigh Dr, Suit 120, Raleigh, NC 27617, USA

Received 31 March 2016, revised 7 July 2016, accepted 11 July 2016
Published online 3 August 2016

Keywords diamond, fluorescence, hydrogen bonds, nanomaterials, Raman spectroscopy, suspensions

* Corresponding author: e-mail vervaljd.aleksey@physics.msu.ru, Phone: +7 (495) 939 16 53, Fax: +7 (495) 939 11 04

Influence of nanodiamonds (ND) of 35 and 100 nm in size, containing NV centers, on the strength of hydrogen bonds under heating of the ND water suspensions in the range of 5–95 °C was studied by Raman spectroscopy. General tendency of both NDs to weaken hydrogen bonds in water was found. Substantial influence of functional state of ND surface on hydrogen bond strength was revealed. An influence of hydrogen bonds on fluorescence properties of the NDs in water suspensions was studied as well. It was found that fluorescence properties of NV centers of 100-nm NDs are stable with regard to change of their surface state, whereas, a fluorescence intensity of the 35-nm NDs essentially depends on strength of hydrogen bonds in the suspension.

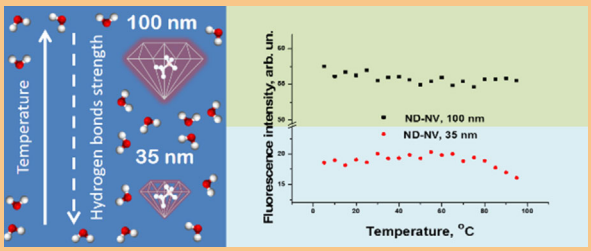

1 Introduction Fluorescent nanodiamonds are promising material for applications in biology and medicine, both, as optical biomarkers and nanosensors [1, 2] and as targeted drug deliverers [3–6]. Of special interest are nanodiamonds (ND) containing color centers, in particular, NV centers. Nanodiamonds with NV centers (ND-NV) possess intense and stable fluorescence under non-resonant excitation, as well as they have large absorption cross section in the optical range, short lifetimes in the excited state, and high quantum yield [7, 8]. These fluorescence properties of ND-NV, as well as the possibility of targeted modification of the ND surface with a view to giving them the properties of an adsorbent or of a drug-carrier, provide wide range of applications for ND-NV in biomedicine. It is obvious that in a biological medium, as a result of interactions of NDs with biomolecules, the properties of both, NDs and their environment, may change. Therefore, in order to find a method for managing the fluorescence and other properties of the NDs and for controlling their impact on the surrounding biomolecules, it is necessary to study mechanisms of the influence of ND and biotissues on each other. As one of the most common interactions in biological tissues is the interaction of molecules through hydrogen bonding, it is expedient to study the interactions on the surrounding molecules in the water.

A special place among the fluorescent ND with color centers is occupied by the ND with NV centers [7–10]. The NV center, which is a point defect of the diamond with C_{3v} symmetry, consists of a nitrogen-vacancy pair, oriented along one of four [111]-type directions of the diamond

lattice [9]. The formation of two types of NV centers – neutral (NV^0) and negatively charged (NV^-) is possible. Both types of the centers are characterized by zero phonon lines (ZPL) at the wavelengths of 638 nm (for NV-center) and of 575 nm (for NV^0-center). In many NDs with NV centers, both types of defects are present and, therefore, both ZPLs appear in the spectra. Both energy states of NV centers are extremely stable and in the volume of the diamond they are never photobleaching. However, by Bradac et al. [11], it was found that the fluorescence of NV centers in small nanodiamonds of 5 nm in size is blinking, and this blinking disappears with aggregation and can be controlled by changes in the diamond surface state. The distance at which NV centers "feel" the surface of the nanodiamond was recently measured using HPHT ND-NV, covered with a diamond layer with SiV centers [12]. The study of fluorescent properties of these particles showed that blinking of the NV centers disappears at distances from the surface larger than 12 nm.

In many studies, both theoretical and experimental, the influence of the functional surface cover on the charge states of near-surface NV centers and, accordingly, on their photoluminescence (PL), were found [13–19]. For example, after the surface modification by hydrogen in the near-surface layer of up to 10 nm, the concentration of positively charged holes increases, which leads, first of all, to the transformation of NV^--center to NV^0-center and, then, to the unknown non-fluorescent state [13, 14]. In Ref. [15] it is shown that the removal of amorphous carbon from the surface of ND-NV, the relative concentration of NV^- centers increases. The reason is that the sp^2-hybridized layer is a trap for electrons, which affects the type of an NV defect and its fluorescence [16].

It is logical to assume that if the functional cover has an impact on the state and amount of NV centers in the ND, then the fluorescence properties of NV centers can be also influenced by the interactions between the surface functional groups with the surrounding molecules of biological tissues or solvents.

Currently, there are many literature data on essential interactions between the ND surface and the surrounding molecules of the solvents, in particular, of water [20–26]. Chakrapani et al. [20] have demonstrated that in an aqueous suspension of the hydrogenated detonation nano-diamonds (DND) occurs regular exchange of electrons between the hydrogen on the surface of ND and water molecules, resulting in absorption or formation of molecular oxygen. This electronic exchange changes the charge sign of the diamond surface. As a result, the electrostatic adhesion between the surface of ND and the solvent molecules reinforces and the water molecules are very actively adsorbed on the surface of ND. The results of studying the DND dispersed in water using synchrotron X-ray scattering and absorption showed that there is electron transfer from the surface of ND to the water [21–23]. Such electronic transitions can affect the optical, colloidal, and chemical properties of DND in water. The influence of the surrounding solvent molecules on the fluorescence properties of dispersed DND was demonstrated by Dolenko and Burikov et al. [24, 25]. There was observed a dependence of the fluorescence intensity of dispersed DND on the amount and strength of hydrogen bonds in water and in protic solvents. As the band of valence vibrations of OH groups is very sensitive to the changes in the number and strength of hydrogen bonds in the solvent [27–30], these studies were performed by Raman spectroscopy of the DND suspensions. It was shown that hydrogen bonds between surface groups of dispersed DNDs with polyfunctional and carboxylated surfaces and water molecules are weaker than hydrogen bonds between molecules of pure water. Parallel studies of suspensions of the DND by fluorescence spectroscopy showed that the weaker and the fewer hydrogen bonds around the DND, the more intense fluorescence of nanoparticles arise in suspension.

This work is devoted to the study of molecular ND-NV interactions in aqueous suspensions by Raman spectroscopy and fluorescence spectroscopy, namely to the study of the effect of dispersed ND on the strength of hydrogen bonds in water, on the one hand, and of the effect of hydrogen bonding on the fluorescence properties of ND-NV, on other hand.

2 Experimental

2.1 Materials In this study, aqueous suspensions of ND with NV centers were investigated. The ND with NV-centers of two sizes, 35 and 100 nm were used (hereinafter ND-NV 35 nm and ND-NV 100 nm). For the preparation of ND-NVs, the HPHT diamonds of 15 μm in size were irradiated with an electron beam with the energy of 2 MeV and a dose of 5×10^{18} e cm^{-2} and were annealed at a temperature of 850 °C for 1 h. The diamond particles were grinded afterwards in a mill with zirconium grains and cleaned with hydrofluoric acid. The fractions of ND-NV of 35 and 100 nm in sizes were separated by centrifugation. Besides, the ND-NVs 35 nm were modified by carboxyl groups by means of treatment in the mixture of sulfuric and nitric acids at a temperature of 70 °C for 4 h.

The following starting aqueous suspensions were prepared: of ND-NV 35 nm at a concentration of 1 g l^{-1}, and of ND-NV 100 nm with a concentration of 2 g l^{-1}.

The aqueous suspensions were prepared by diluting the original suspensions with double-distilled deionized water. Table 1 shows the characteristics of aqueous suspensions of studied ND (Table 1). The dimensions of ND were determined by dynamic light scattering (DLS) on the analyzer ALV-CGS-5000/6010 (Langen, Germany). The zeta potential of the suspension was measured by zeta-sizer Malvern Instruments.

2.2 IR absorption spectroscopy of the studied NDs In order to characterize the surfaces of the studied ND, the IR absorption spectra of vaporized samples of ND were obtained using IR spectrometer Varian 640-IR FT-IR

Table 1 Characteristics of water suspensions of studied NDs.

ND	concentration of ND in starting water suspension ($g\,l^{-1}$)	zeta-potential (mW)	size (nm)
ND-NV 35 nm	1	-40.0 ± 3.2	35 ± 3
ND-NV 100 nm	2	-35.0	100 ± 3

(Fig. 1) with ATR module with ZnSe crystal. The spectral resolution was $4\,cm^{-1}$.

As it can be seen from Fig. 1, measured spectra of both NDs have the following common features: broad band of valence vibrations of O–H in the region 3000–3700 cm^{-1}, band of valence vibrations of C–H in the region 2800–3000 cm^{-1}, band of deformation vibrations of O–H groups near 1640 cm^{-1}, broad band of valence vibrations of C–O–C with a maximum near 1110 cm^{-1}.

Significant differences in the surface cover between 35 and 100-nm ND-NV was found by IR spectroscopy. In the IR spectrum of the ND with the size of 35 nm, the line of valence vibrations of C=O groups is present near 1800 cm^{-1} (Fig. 1), confirming the modification of the surface of this ND by carboxyl groups. The shift of the absorption of the vibration line of C=O from the expected 1750–1760 cm^{-1} to higher frequencies in the region of 1800 cm^{-1} is due to formation of such groups as –C(O)–O–C(O)– and $(–O–)_2C=O$. In the IR spectra of the ND-NV 100 nm there are intense lines of the polycrystalline graphite near 1370–1390 and near 1580 cm^{-1} (Fig. 1). In the IR spectra of smaller ND-NV, these lines are barely visible because the surface of the ND-NV 35 nm had undergone purification and modification of carboxyl groups.

2.3 Laser spectrometer The excitation of the Raman scattering and of the fluorescence of aqueous ND suspensions was performed with the argon laser (a wavelength of 514.5 nm and a power of 130 mW). The spectra were recorded at 90-degree geometry in the range of 550–800 nm. The spectral registration system consisted of a monochromator (Acton 2500i, the focal length of 500 mm, the grating 900 grooves per mm) and a CCD-camera (Jobin Yvon, Synapse 1024 128 BIUV-SYN). For the suppression of the scattering at the unshifted frequency, an interference filter Semrock was used. The thermal stabilization system, based on the Peltier element, allowed to control the sample temperature to within 0.2 °C. All spectra were normalized to the laser power and the sensitivity of detector.

3 Results and discussion

3.1 Temperature dependence of Raman and fluorescence spectra of water suspension of ND The influence of the ND suspended in water on hydrogen bonds of the solvent was studied. For this purpose, a comparative analysis of the changes in the strength of hydrogen bonds in pure water and water suspensions of ND with increasing the samples temperature was performed. It is known that with the temperature increase, the hydrogen bonds in water are significantly weakened [27, 29]. Temperature dependences of the Raman spectra of water and water suspensions for both ND-NV samples at concentrations of $1\,g\,l^{-1}$ for the 35-nm ND and $0.1\,g\,l^{-1}$ for the 100-nm ND were obtained. The temperature of the samples varied from 5 to 95 °C with the step of 5 °C. Such concentrations of ND-NV were chosen due to the selection of the ratio of fluorescence intensities of ND and the water valence band to correct calculation of the χ_{21} parameter (see below).

Figure 2 shows Raman and fluorescence spectra of the $1\,g\,l^{-1}$ water suspension of the ND-NV 35 nm at different temperatures. An intense band in the region of 606–636 nm

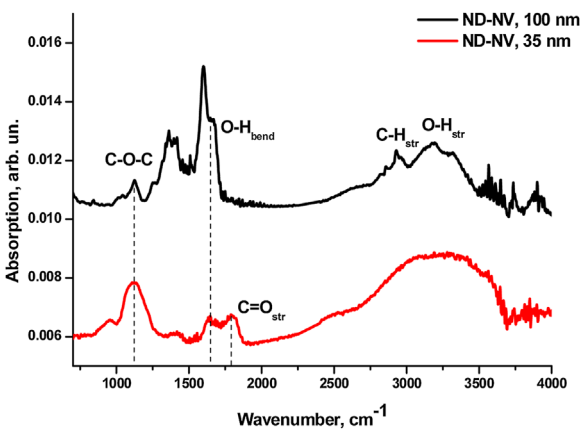

Figure 1 The IR absorption spectra of ND with NV centers with size of 100 and 35 nm, vaporized from aqueous suspensions.

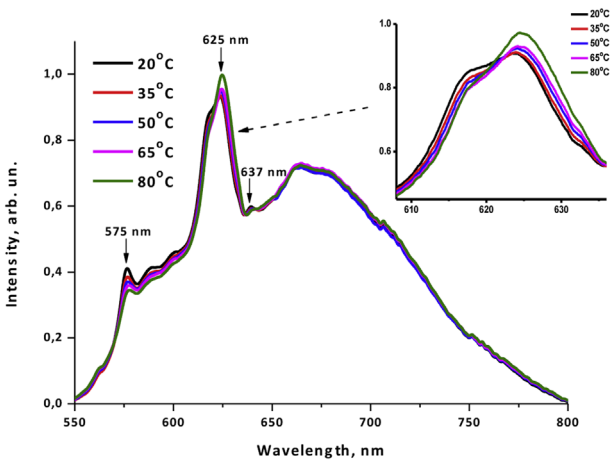

Figure 2 Raman and fluorescence spectra of $1\,g\,l^{-1}$ water suspension of ND-NV 35 nm at different temperatures.

with a maximum at 625 nm is a valence band of the OH groups of water. A broad band in the range of 550–800 nm is a fluorescence spectrum of the ND related to the NV centers. The peak at 575 nm is due to the ZPL of NV^0, while the peak at 638 nm, due to the ZPL of NV^-. The figure shows that in the NDs both, NV^0 and NV^- centers are present.

The band of valence vibrations of OH groups in the Raman spectrum of water is very sensitive to the changes in strength of the hydrogen bonds in solutions [27–30]. Experimental data show that with increasing temperature, the intensity of high-frequency component of the OH valence band increases, and of the low-frequency component – falls, the band maximum shifts to higher frequencies, and the half-width of the whole band reduces [27, 29]. Such a behavior of the water valence band can be explained by the fact that the strength of the hydrogen bonds decreases with temperature increase. The weakening of the hydrogen bonds between the molecules leads to the increase of the frequency of the valence vibrations of OH groups, and of the intensity of high-frequency component of the valence band. These changes are manifested in the behavior of the water valence band under the temperature variations (Fig. 2).

For a quantitative analysis of the changes in the forces of hydrogen bonds in water suspensions, the parameter $\chi_{21} = I_2/I_1$, equal to the ratio of the intensities of a high-frequency and a low-frequency component of the valence band (see inset in Fig. 3) was introduced [25, 29, 30]. It is assumed [27–30] that the high-frequency component of the valence band (with a maximum I_2) is caused by vibrations of the hydroxyl groups with weak hydrogen bonds, and the low-frequency component (with a maximum I_1) – by vibrations of OH groups with strong hydrogen bonds. Therefore, the introduced parameter χ_{21} characterizes the share of weakly bounded OH groups in the solution in relation to the strongly bounded OH groups. That means the growth of the χ_{21} value leads to the weakening of hydrogen bonds in the suspension.

As a quantitative characterization of the fluorescence properties of the ND in aqueous suspensions, the fluorescence parameter $F_0 = S_2/S_1$ (Fig. 3), equal to the ratio of the area of ND fluorescence, phonon lines including, to the area of the valence band of OH groups, was used. In this case, the valence band is used as an internal reference point. In order to highlight the valence band of water from the Raman and fluorescence spectra, the fluorescence signal under the valence band was approximated by a straight line, and subtracted as it is shown in Fig. 3.

3.2 Influence of nanodiamonds with NV centers on hydrogen bonds in water suspensions

For all the obtained Raman spectra from water suspensions in the temperature range of 5–95 °C, the parameter χ_{21} was calculated. Temperature dependence of the $\chi_{21}(T)$ parameter for the valence bands of water and water suspensions of 35- and 100-nm NDs are shown in Fig. 4.

The following conclusions can be drawn from the obtained data:

(1) The χ_{21} (T) dependencies for both types of the ND-NV do not coincide with that for pure water. This means that both NDs change the strength of the hydrogen bonds in the water in addition to the changes in hydrogen bonds therein caused by the temperature changes.

(2) The χ_{21} (T) dependencies for the ND-NV 35 nm and for pure water are almost identical for up to the 80° C, and only at higher temperatures the values of χ_{21} for the ND-NV suspensions become slightly higher than for the water. This means that the presence of carboxyl groups on the surface of ND generates a hydration shell around the ND with slightly less strong hydrogen bonds than in the water. Under the temperatures greater than 80 °C, this "looseness" of the hydrogen bonds around the carboxylated ND become stronger and manifests in the $\chi_{21}(T)$ dependence. These results confirm our data obtained previously during the study of the influence of

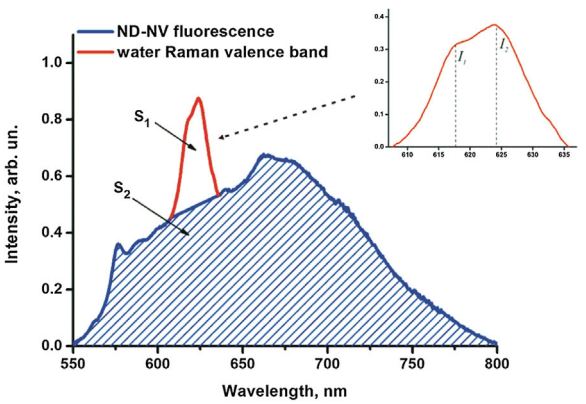

Figure 3 Illustration of calculation of χ_{21} and F_0 parameters by fluorescence and Raman spectra of water suspensions of ND-NV: $\chi_{21} = I_2/I_1$; $F_0 = S_2/S_1$.

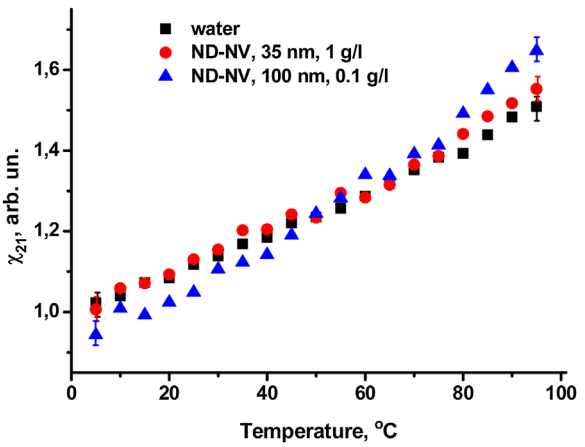

Figure 4 Temperature dependences of χ_{21} parameter for the valence vibrations bands of OH groups in water and water suspensions of ND with NV centers.

detonation NDs with various functional covers on the hydrogen bonds in water [25].

(3) The $\chi_{21}(T)$ dependences for the ND-NV 100 nm significantly differ from those for smaller NDs and pure water. Thus, for example, the χ_{21} values for the NDs of larger sizes are much lower than for smaller NDs and pure water at the temperatures up to 50 °C. At temperatures greater than 70 °C, there is a growth of the χ_{21} parameter of ND-NV 100 nm and a significant excess of its values compared to the χ_{21} values for the other ND and pure water. This means that despite a lower concentration and a lower total surface area of the nanoparticles, the ND-NV 100 nm much stronger change hydrogen bonding forces in suspension than the ND-NV 35 nm. Moreover, at low temperatures (up to 50 °C) they significantly increase hydrogen bonding in water, and at high temperatures (over 70 °C), significantly weaken them. Such a difference in the effect on hydrogen bonds in water for two ND-NVs is explained by different functional cover of these NDs. As demonstrated by the IR absorption spectroscopy of the studied samples (Fig. 1), on the surface of 100-nm NDs there is a considerable amount of nanographite, which adsorbs hydroxyl groups of water molecules. As a result, around the ND-NV 100 nm, a thick hydrate shell with strong hydrogen bonds is formed. Under the heating of the suspension, this shell is destroyed, while under a further increase in temperature (above 70 °C), hydrogen bonds in the ND environment are actively weakened.

Thus, the influence of the suspended ND on the structure of the solvent largely depends on their functional covering. Despite the lower concentration (10 times) and smaller total surface area (29 times), the ND-NV 100 nm with a large number of graphite on the surface much stronger modify hydrogen bonding in water than ND-NV 35 nm modified by carboxyl groups.

It should be noted that if we estimate the number of water molecules close to the NDs surface in our suspensions (e.g.,, in the surrounding layer of water molecules 2–5 nm thick), we obtain an unexpectedly small fraction of water molecules directly interacting with the surface of NDs: less than 0.1% of all water molecules in aqueous suspension of 35-nm ND with concentration of 1 g l^{-1}. Nevertheless, our parameter χ_{21} is sensitive to structural changes in water in such suspensions.

In the case of Raman spectroscopy, we considered the frequency changes of intramolecular vibrations of water molecules in the volume of the aqueous suspension of NDs. Even if water molecules are not in the close proximity (i.e., not under the direct influence) of nanoparticles, the hydrogen bonds between them can be changed by adjustment and reorientation of the neighboring molecules. Thus, the frequencies of stretching vibrations of these molecules are also changed under the influence of modified hydrogen bonds. Due to the high polarity of water molecules such changes in hydrogen bonds can spread far from the nanoparticles.

Some results of the study of aqueous suspension of NDs also demonstrate "abnormal" properties of such suspensions. In the study [26], the authors made the following conclusion: "Thus, even tiny concentrations of DND in water greatly enhance its ε (the dielectric constant), suggesting that DND particles may cause structural rearrangement in water at surprisingly large distances, probably by the mechanism of orientational polarization."

Therefore, it should be understood that changes of the stretching bands that we observed reflect the changes in the frequencies of stretching vibrations of water molecules not in the area of direct influence of NDs but in the volume of NDs suspensions – both next to the NDs and far from them.

3.3 Fluorescence properties of ND-NV in water The effect of the changes in the strength of hydrogen bonds in water on the fluorescence properties of the NDs was studied by the analysis of the obtained temperature dependences for the ND fluorescence spectra.

Figure 5 shows fluorescence and Raman spectra of the studied water suspensions at 25 °C. It should be noted that despite the 10-times less total volume per unit suspension volume of ND-NV 100 nm, the intensity of the fluorescence of these nanoparticles is greater than the fluorescence intensity of ND-NV 35 nm. It can be assumed that under crushing of the irradiated diamond (both NDs are obtained by crushing of the same irradiated diamond) because of the size and surface difference of the NDs the effective number of NV^- centers has decreased more for the smaller particles. As a result, the fluorescence intensity of ND-NV with the size of 35 nm is less in comparison with the intensity of the ND-NV with the size of 100 nm.

For the quantitative analysis of the dependence of the ND fluorescence properties on the temperature of the samples (i.e., on the strength of hydrogen bonds, the

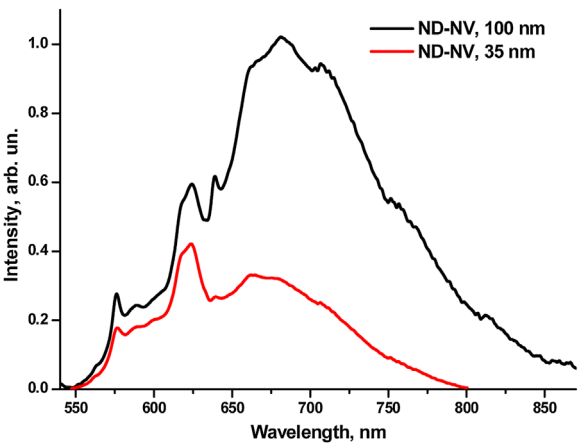

Figure 5 Fluorescence and Raman spectra of ND-NVs in water at a temperature of 25 °C. The spectra are normalized to the area of the valence band.

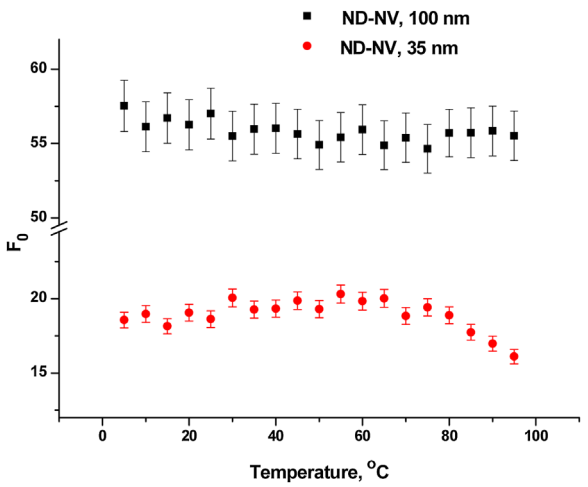

Figure 6 Dependence of the F_0 parameter of water suspensions of NDs with NV centers on the temperature.

fluorescence parameter F_0, equal to the ratio of the ND fluorescence area, phonon lines including, to the area of the valence band of the water, was calculated (Fig. 3). Figure 6 shows the obtained dependences of the F_0 parameter on the temperature of water suspensions of both ND-NV samples.

As seen from Fig. 6, with the temperature change, the fluorescence intensity of ND-NV 100 nm remains practically unchanged in water. Thus, the large NDs demonstrate high degree of independence of fluorescence of NV centers from the changes in hydrogen bonding strength in the solvent, although the NDs themselves affect significantly on hydrogen bonds (see above). In contrast, for the suspension of ND-NV 35 nm, the dependence of fluorescence on the hydrogen bonding strength is observed. At the temperatures above 70 °C, the fluorescence intensity of smaller ND-NVs decreases (Fig. 6). Given that with increasing temperature, the hydrogen bonds are weakened (Fig. 4), we can conclude that the reduction of the hydrogen bonds in the ND-NV 35 nm solution changes the surface state of ND in a such manner that the NV-centers in the near-surface layer lose their fluorescence properties.

The obtained results are in good agreement with the conclusions of Shershulin et al. [12], where the authors investigated the fluorescence of O-terminated nanodiamonds with NV centers synthesized by HPHT, on which the diamond layers of different thickness were grown by a CVD-method. From a comparison of such diamond structures with different thickness of the outer layer, the authors concluded that the NVs "feel" the surface of NDs at a distance up to 12 nm which causes the "blinking" of fluorescence of the color centers.

4 Conclusions Both an influence of ND with NV centers on the structure of the solvent in water suspensions, and an influence of structure of the solvent on fluorescence properties of ND was studied using Raman spectroscopy. The water suspensions of NDs different sizes (35 and 100 nm) and various surface state were studied. It was found that influence of suspended NDs on the strength of hydrogen bonds significantly depends on the ND functional cover. Despite lower concentration (10 times) and lower total surface area (29 times), 100-nm ND with larger amount of graphite on the surface have stronger influence on hydrogen bonds in water in comparison with 35-nm NDs modified by carboxylic groups. The weakening of hydrogen bonds in the surroundings of 35-nm ND was found to change the surface state of NDs in such a way that NV-centers in the subsurface layer lose their fluorescence properties. A dependence of fluorescence properties of 100-nm NDs on the strength of hydrogen bonds was not revealed.

Acknowledgements This work was supported in part by the grant of the Russian Science Foundation no. 14-12-01329 (I.V., S.B.), by the grant of the Russian Foundation for Basic Research no. 15-29-01290 ofi_m (T.D., A.V.), by the grant of the Russian Foundation for Basic Research no. 16-32-00882_mol_a (K.L.), by the Russian Ministry of Science and Education Project (project ID RFMEFI60414 × 0082) (N.B.), by the National Institute of Health under SBIR Contract 268201500010C-0-0-1 (O.Sh.). This work was done in accordance with the Competitiveness Program of NRNU MEPhI.

References

[1] A. Krueger, Chem. Eur. J. **14**, 1382 (2008).
[2] V. Vaijayanthimala, P.-Y. Cheng, S.-H. Yeh, K.-K. Liu, C.-H. Hsiao, J.-I. Chao, and H.-C. Chang, Biomaterials **33**(31), 7794 (2012).
[3] M. Chen, E. D. Pierstorff, R. Lam, S. Y. Li, H. Huang, E. Osawa, and D. Ho, ACS Nano **7**(3), 2012 (2009).
[4] K. K. Liu, W. W. Zheng, C. C. Wang, Y. C. Chiu, C. L. Cheng, Y. S. Lo, C. Chen, and J. I. Chao, Nanotechnology **21**, 315106 (2010).
[5] N. Prabhakar, T. Nareoja, E. von Haartman, D. S. Karaman, H. Jiang, S. Koho, T. Dolenko, P. Hanninen, D. I. Vlasov, V. G. Ralchenko, S. Hosomi, I. I. Vlasov, C. Sahlgren, and J. M. Rosenholm, Nanoscale **5**(9), 3713 (2013).
[6] R. Lam and D. Ho, Expert Opin. Drug Deliv. **6**(9), 883 (2009).
[7] F. Jelezko and J. Wrachtrup, Phys. Status Solidi A **203**(13), 3207 (2006).
[8] M. W. Doherty, N. B. Manson, P. Delaney, F. Jelezko, J. Wrachtrup, and L. C. L. Hollenberg, Phys. Rep. **528**, 1 (2013).
[9] G. Davies and M. F. Hamer, Proc. R. Soc. London A **348**, 285 (1976).
[10] C. Kurtsiefer, S. Mayer, P. Zarda, and H. Weinfurter, Phys. Rev. Lett. **85**, 290 (2000).
[11] C. Bradac, T. Gaebel, N. Naidoo, M. J. Sellars, J. Twamley, L. J. Brown, A. S. Barnard, T. Plakhotnik, A. V. Zvyagin, and J. R. Rabeau, Nature Nanotechnol. **5**, 345 (2010).
[12] V. A. Shershulin, V. S. Sedov, A. Ermakova, U. Jantzen, L. Rogers, A. A. Huhlina, E. G. Teverovskaya, V. G. Ralchenko, F. Jelezko, and I. I. Vlasov, Phys. Status Solidi A **212**, 2600 (2015).
[13] M. V. Hauf, B. Grotz, B. Naydenov, M. Dankerl, S. Pezzagna, J. Meijer, F. Jelezko, J. Wrachtrup, M. Stutzmann,

F. Reinhard, and J. A. Garrido, Phys. Rev. B **83**, 081304(R) (2011).
[14] V. Petrakova, A. J. Taylor, I. Kratochvilova, F. Fendrych, J. Vacik, J. Kucka, J. Stursa, P. Cigler, M. Ledvina, A. Fiserova, P. Kneppo, and M. Nesladek, Adv. Funct. Mater. **22**, 812 (2012).
[15] L. Rondin, G. Dantelle, A. Slablab, F. Grosshans, F. Treussart, P. Bergonzo, S. Perruchas, T. Gacoin, M. Chaigneau, H.-C. Chang, V. Jacques, and J.-F. Roch, Phys. Rev. B **82**, 115449 (2010).
[16] A. R. Kirmani, W. Peng, R. Mahfouz, A. Amassian, Y. Losovyj, H. Idriss, and K. Katsiev, Carbon **94**, 79 (2015).
[17] H. Pinto, R. Jones, D. W. Palmer, J. P. Goss, Amit K. Tiwari, P. R. Briddon, Nick G. Wright, Alton B. Horsfall, M. J. Rayson, and S. Öberg, Phys. Rev. B **86**, 045313 (2012).
[18] V. Petrakova, M. Nesladek, A. Taylor, F. Fendrych, P. Cigler, M. Ledvina, J. Vacik, J. Stursa, and J. Kucka, Phys. Status Solidi A **208**(9), 2051 (2011).
[19] W. Hu, Z. Li, and J. Yang, Comput. Theoret. Chem. **1021**, 49 (2013).
[20] V. Chakrapani, J. C. Angus, A. B. Anderson, S. D. Wolter, B. R. Stoner, and G. U. Sumanasekera, Science **318**, 1424 (2007).
[21] T. Petit, H. A. Girard, A. Trouvé, I. Batonneau-Gener, P. Bergonzo and J.-C. Arnault, Nanoscale **5**, 8958 (2013).
[22] T. Petit, M. Pflüger, D. Tolksdorf, J. Xiao, and E. F. Aziz, Nanoscale **7**, 2987 (2015).
[23] T. Petit, H. Yuzawa, M. Nagasaka, R. Yamanoi, E. Osawa, N. Kosugi, and E. F. Aziz, J. Phys. Chem. Lett. **6**, 2909 (2015).
[24] T. A. Dolenko, S. A. Burikov, K. A. Laptinskiy, J. M. Rosenholm, O. A. Shenderova, and I. I. Vlasov, Phys. Status Solidi A **212**(11), 2512 (2015).
[25] T. A. Dolenko, S. A. Burikov, J. M. Rosenholm, O. A. Shenderova, and I. I. Vlasov, J. Phys. Chem. C **116**, 24314 (2012).
[26] S. S. Batsanov, E. V. Lesnikov, D. A. Dankin, and D. M. Balakhanov, Appl. Phys. Lett. **104**, 133105 (2014).
[27] G. E. Walrafen, M. R. Fisher, M. S. Hokmabadi, and W.-H. Yang, J. Chem. Phys. **85**(12), 6970 (1986).
[28] P. Terpstra, D. Combes, and A. Zwick, J. Chem. Phys. **92**(1), 65 (1989).
[29] T. A. Dolenko, I. V. Churina, V. V. Fadeev, and S. M. Glushkov, J. Raman Spectrosc. **31**, 863 (2000).
[30] S. A. Burikov, T. A. Dolenko, P. A. Velikotnyi, A. V. Sugonyaev, and V. V. Fadeev, Opt. Spectrosc. **98**(2), 235 (2005).